Underestimation of the Tambora effects in North American taiga ecosystems

Environmental Research Letters

LETTER

Underestimation of the Tambora effects in North American taiga ecosystems

Fabio Gennaretti[1,2,9], Etienne Boucher[3], Antoine Nicault[4], Guillermo Gea-Izquierdo[5], Dominique Arseneault[6], Frank Berninger[7], Martine M Savard[8], Christian Bégin[8] and Joel Guiot[1]

[1] Aix Marseille University, CNRS, IRD, Coll France, CEREGE, Aix-en-Provence, 13545, France
[2] Université de Lorraine, AgroParisTech, INRA, UMR1434 Silva, Nancy, 54000, France
[3] Département de Géographie and GEOTOP, Université du Québec à Montréal, Montréal, H3C3P8, Canada
[4] Aix Marseille University, CNRS, ECCOREV, Aix-en-Provence, 13545, France
[5] Departamento de Sistemas y Recursos Forestales, INIA-CIFOR, Madrid, 28040, Spain
[6] Département de Biologie, Chimie et Géographie, Université du Québec à Rimouski, Rimouski, G5L3A1, Canada
[7] Department of Forest Sciences, University of Helsinki, Helsinki, 00014, Finland
[8] Geological Survey of Canada, Natural Resources Canada, G1K9A9, Québec, Canada
[9] Author to whom any correspondence should be addressed.

E-mail: fabio.gennaretti@inra.fr

Keywords: tambora legacy, Eastern Canada, regional climate responses, terrestrial biosphere responses, forest demography, mechanistic understanding, process-based modeling

Supplementary material for this article is available online

OPEN ACCESS

RECEIVED
12 October 2017

REVISED
3 January 2018

ACCEPTED FOR PUBLICATION
31 January 2018

PUBLISHED
23 February 2018

Abstract

The Tambora eruption (1815 AD) was one of the major eruptions of the last two millennia and has no equivalents over the last two centuries. Here, we collected an extensive network of early meteorological time series, climate simulation data and numerous, well-replicated proxy records from Eastern Canada to analyze the strength and the persistence of the Tambora impact on the regional climate and forest processes. Our results show that the Tambora impacts on the terrestrial biosphere were stronger than previously thought, and not only affected tree growth and carbon uptake for a longer period than registered in the regional climate, but also determined forest demography and structure. Increased tree mortality, four times higher than the background level, indicates that the Tambora climatic impact propagated to influence the structure of the North American taiga for several decades. We also show that the Tambora signal is more persistent in observed data (temperature, river ice dynamics, forest growth, tree mortality) than in simulated ones (climate and forest-growth simulations), indicating that our understanding of the mechanisms amplifying volcanic perturbations on climates and ecosystems is still limited, notably in the North American taiga.

Introduction

On 10 April 1815, the Tambora volcano, located in the Sumbawa island in Indonesia, entered into the culminating phase of a large Plinian eruption which had huge local and global impacts on climate, the environment and human societies (Harington 1992, Oppenheimer 2003, Raible *et al* 2016). Massive injection of at least 60 teragrams (Tg) of SO_2 into the atmosphere produced stratospheric sulfate aerosols which decayed in concentration over three years and shielded the earth from incoming solar radiation (Self *et al* 2004). Consequently, global land temperatures dropped by about 1 °C in 1816, which is known as the 'year without a summer', and remained low for 6–10 years according to simulation studies (Raible *et al* 2016). This climatic perturbation occurred during a period of reduced solar irradiance (Dalton minimum) which was also impacted by other strong volcanic eruptions (Wagner and Zorita 2005), thus culminating in one of the coldest episodes of the 'Little Ice Age'.

Although the Tambora eruption is quite recent in historical terms, its impacts are much better constrained in Europe than elsewhere because of the denser network of historical sources, proxy records and early meteorological stations (Brugnara *et al* 2015). Furthermore, many discrepancies exist on the intensity and duration of the Tambora climatic impact as

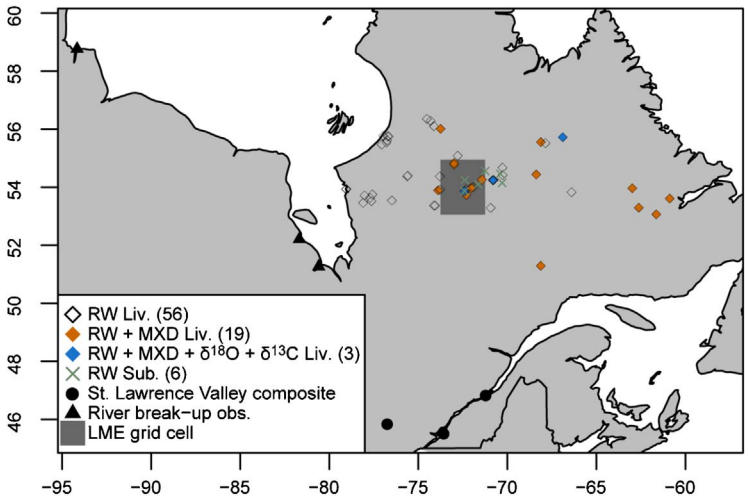

Figure 1. Data location. The number of sites with specific tree-ring proxy records is within brackets. RW Liv. is ring width chronologies from living trees, RW Sub. is ring width chronologies from subfossil trees, MXD is ring maximum density chronologies, LME is Last Millennium Ensemble.

detected by different observed (e.g. weather observations, tree-ring proxies) and simulated records (Büntgen *et al* 2015). These discrepancies remain largely unexplained because of the poor mechanistic understanding of the responses of the climate and the biosphere at the regional level. For example, the Tambora impact on the carbon cycle is poorly understood. The atmospheric CO_2 concentration was slightly reduced for 15 years after the Tambora erupted (MacFarling Meure *et al* 2006), likely because the carbon uptake over land increased. This was driven by the lower temperatures, which could have reduced ecosystem respiration in northern latitudes and increased net primary production in the tropics (Tjiputra and Otterå 2011, Kandlbauer *et al* 2013). However, there is no consensus on the terrestrial biosphere responses and associated mechanisms at regional level (Raible *et al* 2016). For example, we do not know how northern forest ecosystems reacted to the Tambora abrupt perturbation in terms of wood biomass assimilation and forest demography (i.e. tree mortality and recruitment), which are significant components of the regional carbon budget.

This paper focuses on the Tambora impacts in Eastern Canada (figure 1) where many individual records and sources show that the volcanic perturbation on climate was particularly strong. The Hudson's Bay Company and the Moravian missionary archives report extremely cold temperatures and thick and persistent sea-ice conditions in the Hudson Bay and along the Labrador coast from October 1815 to March 1818, at the beginning of a generally cold 60 year period (Wilson 1992, D'Arrigo *et al* 2003). These harsh climatic conditions contributed to poor hunting success, crop failure and famines afflicting native people, as well as European traders and colonists from Ontario to the Labrador coast (Suffling and Fritz 1992, D'Arrigo *et al* 2003). In southern Quebec, severe winters between 1816 and 1819 caused the formation of exceptional ice bridges on the St. Lawrence River near Quebec City for four consecutive years (Houle *et al* 2007). The Tambora impact in Eastern Canada is also visible in biological proxy records. The lowest 1816 anomalies recorded in a Northern Hemisphere network of tree-ring density measurements come from the Quebec-Labrador Peninsula (Briffa *et al* 1998). Simultaneously and in the same region, we detect the beginning of a 40 year regime shift to the lowest values of the last millennium in ring width chronologies (Gennaretti *et al* 2014c). Unfavorable climatic conditions during the first half of the 19th century are also detectable in pollen datasets (Viau *et al* 2012), $\delta^{18}O$ cellulose of Sphagnum mosses (Bilali *et al* 2013), and reconstructions of spruce height growth (Vallée and Payette 2004). These climatic, historical and biological impacts are in line with the idea, corroborated by model simulation experiments, that Eastern Canada may be especially sensitive to volcanic forcing, if an amplification by subsequent North Atlantic sea-ice-ocean feedbacks takes place (Otterå *et al* 2010, Miller *et al* 2012). However, a comprehensive study merging several kinds of observed and simulated annually-resolved data from Eastern Canada during the Tambora time has yet to be carried out.

Here, we present an extensive network composed of early meteorological observations, climate simulations, and river and tree-ring proxy records to analyze the Tambora impacts in Eastern Canada. We evaluate the propagation of the of the Tambora signal through the regional climate and the forest ecosystems. As it has been shown for other regions or at the global scale (Segschneider *et al* 2013, Büntgen *et al* 2015), we hypothesize that the persistence of volcanic signals in biological records and in ecosystem carbon uptake may be longer than in the climate system. We also reconstruct tree mortality in the Eastern Canadian taiga during the early 19th century to analyze whether the Tambora eruption severely affected forest demography

and structure with long-term consequences. We then discuss the mechanisms that could have amplified the volcanic impact and that are not taken into account by ecophysiological models. Finally, we compare the likely impacts on forest carbon uptake of Tambora-like eruptions simulated under past (early 19th century) and current (last decades) climate conditions.

Materials and methods

Hydroclimate observations

We collected observed data from early meteorological records and annals of river break-up dates. The meteorological records come from historical and modern observations from several observers and three locations in Southern Quebec: Montreal, Quebec City and Fort Coulonge (figure 1). These observations were compiled by Slonosky (2014, 2015), www.ncdc.noaa.gov/paleo-search/study/16336 into two unique time series for the St. Lawrence Valley of daily minimum and maximum temperature values. Here we used the mean of the two time series over the 1803–2010 period (St. Lawrence Tmean hereafter). The river break-up dataset consists of the first break-up dates of river estuaries on the west coast of the Hudson and James Bays in the 18th and 19th centuries. These data were compiled by Moodie and Catchpole (1975) and used in a regional multi-proxy climate reconstruction (Guiot 1985). We retained three rivers and locations with more complete data over the 1736–1866 period: Churchill Factory, Fort Albany and Moose Factory (figure 1, dataset S1 available at stacks.iop.org/ERL/13/034017/mmedia).

Simulated climate

Thirteen climate simulations with all transient forcings of the Last Millennium Ensemble project (LME; Otto-Bliesner *et al* 2016, www.cesm.ucar.edu/projects/community-projects/LME/) were used to further evaluate the temporal and spatial climate impacts of the Tambora eruption over Eastern Canada. The LME offers the possibility to analyze a large ensemble of simulations varying for initial conditions (background state of the climate system at the beginning of the model runs) but conducted with the same up-to-date model version (CESM-CAM5_CN developed primarily at the National Center for Atmospheric Research) and using the same set of forcings over the 850–2005 period. In this way, we limit uncertainties due to the use of different models and forcing records which would complicate our analysis, but at the same time we can explore the natural forcing and internal variability of the climate system with multiple simulations. For each simulation, we extracted the following climate variables: reference height (two meters) mean-maximum-minimum temperature, total precipitation and net solar flux at surface. These data were used to produce annual time series plots, monthly anomalies plots, and maps. A simple post-processing method was applied to the data of the grid node in the middle of our study region in Eastern Canada (figure 1). This consisted in correcting each variable by the difference between its 1950–2005 average and the average value in the NRCan observational dataset (the gridded interpolated Canadian database of daily minimum–maximum temperature and precipitation for 1950–2015; Hutchinson *et al* 2009, http://cfs.nrcan.gc.ca/projects/3/4).

Tree-ring proxies and forest carbon

An extensive network of tree-ring temperature-sensitive proxy records covering the central Quebec-Labrador peninsula and always including the 1800–1850 period was assembled to analyze the Tambora impact in Eastern Canada (figure 1). This network includes data from living and subfossil spruce trees. All records from living trees go back at least to 1800 AD and come from Nicault *et al* (2014a, 2014b) and Naulier *et al* (2015), namely, 56 ring width chronologies (hereafter RW Liv.) calculated using the age-band standardization method (Briffa *et al* 2001), 19 maximum density chronologies (MXD) and three $\delta^{18}O$ and $\delta^{13}C$ chronologies (rings were sampled at a two-year resolution for the isotopic chronologies). Additionally, ring width data were derived from subfossil black spruces (tree remains into lakes) collected from six sites (Gennaretti *et al* 2014c). These data were assembled into six site-specific and two cambial age-specific chronologies covering the 910–2011 period (RW Sub.) using the regional curve standardization pivot correction method which was designed to reduce the impact of varying sampling heights in the used material (Autin *et al* 2015). Decadal tree-mortality rates at these same six sites were reconstructed from the outermost tree-ring dates of the subfossil trees. However, it must be noted that the outermost tree-rings are eroded with the time (Gennaretti *et al* 2014b) and that, as a consequence, the retrieved dates of tree deaths are antedated by some years.

The impact of the Tambora eruption on boreal forest aboveground carbon assimilation in eastern Canada was firstly evaluated through the computation of a wood biomass production index (MWI; $g\,yr^{-1}$, Boucher *et al* 2017) at the 19 sites where both tree-ring width and density measurements were available:

$$\begin{aligned} &\text{For thin slice of wood} \rightarrow \mathrm{BVI}_t \propto \mathrm{BAI}_t \\ &\mathrm{MWI}_t = \mathrm{BVI}_{\mathrm{BW}(t)} \times D_{\mathrm{EW}(t)} + \mathrm{BVI}_{\mathrm{LW}(t)} \times \\ &D_{\mathrm{LW}(t)} \end{aligned} \quad (1)$$

where BVI is the basal volume increment (cm^3), BAI is the basal area increment (cm^2), D is the wood density ($g\,cm^{-3}$), and EW and LW are the earlywood and the latewood fractions, respectively. Secondly, the MAIDEN ecophysiological forest model (Misson 2004, Gea-Izquierdo *et al* 2015), recently adapted for boreal black spruce sites (Gennaretti *et al* 2017), was used to simulate the forest gross primary production (GPP) in the study region in Eastern Canada

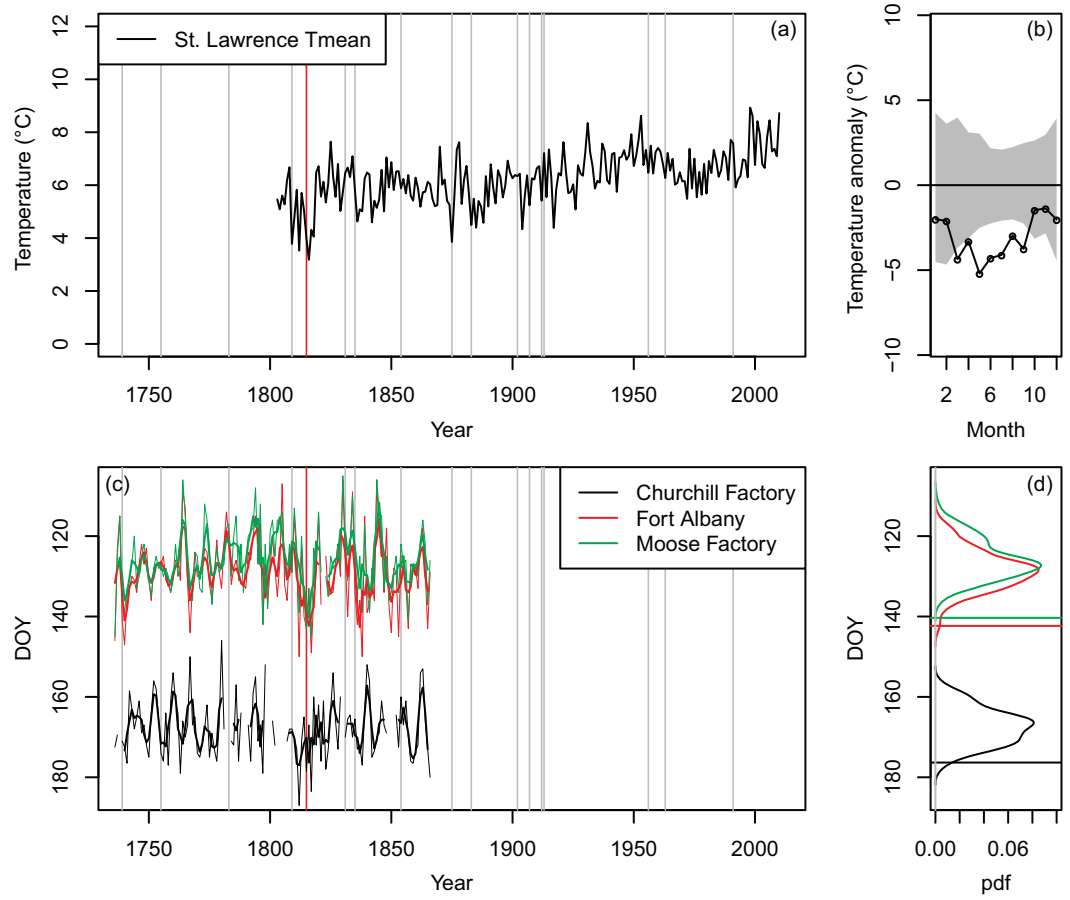

Figure 2. Hydroclimate observations. St. Lawrence annual Tmean time series (*a*) and 1816 monthly anomalies ((*b*); black: 1816 anomalies, grey: 90% confidence intervals computed with data over the 1803–1814 and 1818–2010 period). River estuaries' first break-up date time series ((*c*); thin lines: annual values, bold lines: three-year running means; note that the *y*-axis is inverted and lower values correspond to later first break-up in spring) and their 1816 anomalies ((*d*); pdfs are empirical probability density functions and are computed with the running mean data over the 1736–1814 and 1818–1866 period, horizontal lines are 1816 values). In (*a*) and (*c*) vertical lines are important eruption years (see table 1; Tambora is in red). DOY is the day of year.

Table 1. Years of large eruptions plotted in the figures and derived from Gao *et al* (2008, global total stratospheric sulfate aerosol injection >15 Tg), Crowley and Unterman (2013, satellite aerosol optical depth >0.1), Esper *et al* (2013, eruptions classified as large events) or Sigl *et al* (2013, 2015, eruptions classified as large events).

Year	Volcano	Location
1739	Shikotsu	Japan
1755	Katla	Iceland
1783	Laki	Iceland
1809	Unknown	Unknown
1815	Tambora	Indonesia
1831	Babuyan	Philippines
1835	Cosiguina	Nicaragua
1854	Shiveluch	Russia
1875	Askja	Iceland
1883	Krakatau	Indonesia
1902	Santa Maria	Guatamala
1907	Ksudach	Russia
1912	Katmai	USA
1913	Colima	Mexico
1956	Bezymianny	Russia
1963	Agung	Indonesia
1991	Pinatubo	Indonesia

during the Tambora time. We used as MAIDEN inputs daily minimum–maximum temperature and precipitation values extracted by the 13 LME simulations and CO_2 concentration data obtained by interpolating to daily resolution the ice core CO_2 record of MacFarling Meure *et al* (2006). The parameters used to run MAIDEN were sampled from their posterior distributions described in Gennaretti *et al* (2017).

Statistical significance of the 1816 anomaly

The significance of the 1816 anomaly just after the 1815 Tambora eruption was verified in all the used datasets by comparing the 1816 values to the distribution of the data excluding the years most impacted by the Tambora (1815–1817). For climate simulations, we also compared the 1816 anomalies in the study area against the distribution of the 1816 anomalies from elsewhere (see figures 2–5).

Results

The large amount of collected data, including hydroclimate observations, climate simulations and tree-ring proxies, is well-spread over Eastern Canada (figure 1). The St. Lawrence annual mean temperature (Tmean) time series indicates that the Tambora eruption induced a significant cooling over three years in

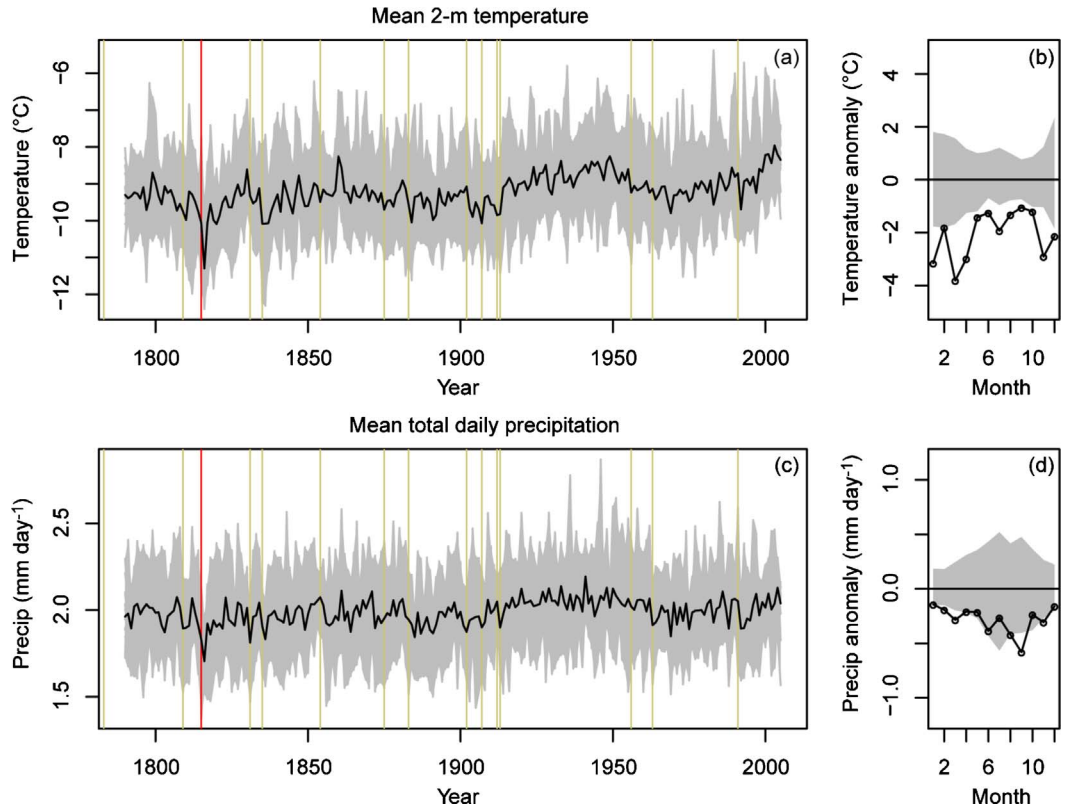

Figure 3. LME simulated values for the grid node in the middle of our study region in Eastern Canada. Mean 2 m temperature annual time series ((*a*); black: mean of the 13 members, grey: inter-member spread) and 1816 monthly anomalies in the mean ensemble time series relative to the monthly-specific median value ((*b*); black: 1816 anomalies, grey: 90% confidence intervals computed with data over the 1790–1814 and 1818–2005 period of the mean ensemble time series). Mean total daily precipitation time series (*c*) and 1816 monthly anomalies (*d*). In (*a*) and (*c*) vertical lines are important eruption years (see table 1; Tambora is in red).

Southern Quebec (1816–1818) with maximum 1816 negative anomalies up to −5 °C in spring and summer (figure 2). At the same time, the first break-up date of the main rivers on the west coast of the Hudson/James Bays was delayed by about 10 d and was especially late in 1817 indicating cold winter/spring conditions (figure 2). Comparatively, climate simulations of the LME project highlight that the Tambora produced negative anomalies in Eastern Canada on both temperature and precipitation time series (figure 3), but these anomalies lasted only one year and the 1816 temperature anomalies were more negative in winter than in summer (the opposite was shown by the St. Lawrence Tmean). The LME simulations also highlight that Eastern Canada was one of the regions of the world displaying the coldest temperature anomalies in 1816 which was a cold year almost everywhere (figures 4(*a*)–(*b*)). These anomalies in Eastern Canada were not associated with a reduction of solar irradiance (figures 4(*e*)–(*f*)), suggesting that they were caused by some climate feedbacks or teleconnections affecting the atmospheric circulation. The 1816 global picture is much more complicated for precipitation anomalies (figures 4(*c*)–(*d*)). Some regions of the world displayed wet anomalies and others displayed dry anomalies, such as Eastern Canada.

Tree-ring proxy records in Eastern Canada were strongly impacted by the Tambora eruption and, to a lesser extent, by the other large eruptions of the first half of the 19th century (figure 5). The strength and the persistence of the impact depend on the proxy. The MXD time series show the lowest indexes in 1816 and 1817, which are followed by fast recovery. Conversely, the RW time series drop down in 1816 and remain low for about 12 years, with the exception of normal growth in 1822. The recovery process was almost completed in 1828 but the 1831 Babuyan and the 1835 Cosiguina eruptions reduced the growth again. A similar response is shown by the isotopic proxies (δ^{18}O and δ^{13}C), with particularly low values in 1824 and 1825 (these years are negative anomalies for all proxies). Although RW data come from a large region in Eastern Canada (figure 1), the behavior of the RW time series (figure 5(*c*)) is extremely consistent whatever the site, the material used (living or subfossil trees), and the tree cambial age (subfossill trees with cambial ages < 50 years or cambial ages $>= 50$ years).

The RW data from subfossil trees allow the analysis of the Tambora impact on tree mortality. These data are extremely robust due to the high sample depth (overall replication always over 200 trees; figure 6(*a*)), which declines up to the Tambora eruption suggesting that a massive tree mortality was likely linked to this event. Figure 6(*b*) indicates that 19% of the trees died in the decade ending in 1815 and 15% in the decade ending in 1805. Note that tree mortality is slightly

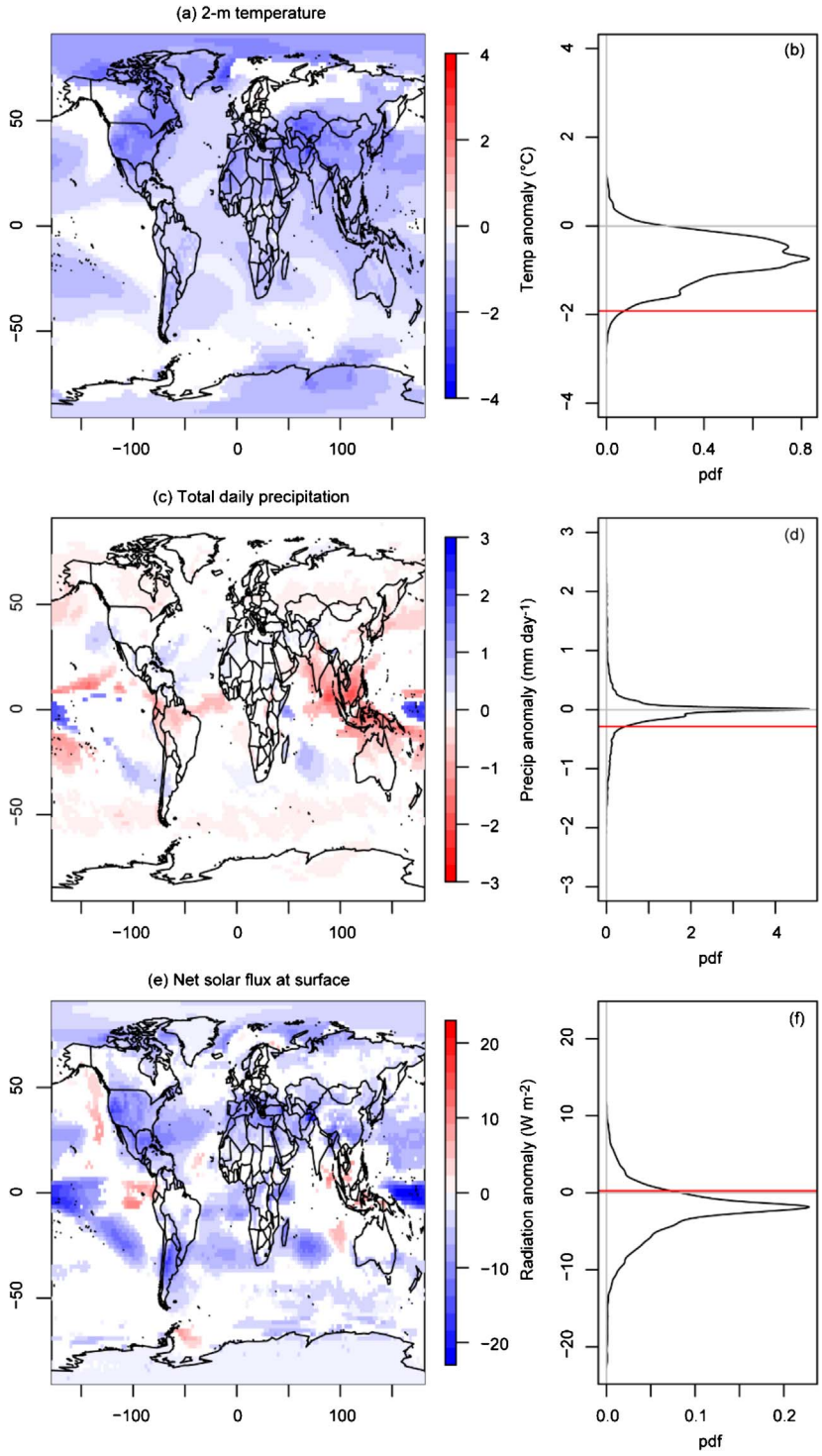

Figure 4. Average 1816 global anomaly fields of the 13 member LME ensemble relative to the 25 year period between 1790 and 1814. We show anomalies of mean 2 m temperature ((*a*); °C), mean total daily precipitation ((*c*); mm day^{-1}), and mean net solar flux at surface ((*e*); W m^{-2}). White areas denote non-significant anomalies (one-sample Wilcoxon test with $p > 0.05$; $n = 13$). In (*b*), (*d*) and (*f*) the value of the grid point in the middle of our study region in Eastern Canada is indicated by a red horizontal line and is compared to the distribution of the values in the maps (PDFs).

antedated here because it is reconstructed with the outermost tree-ring dates and subfossil trees lose, through erosion, an average of 3.2 outermost rings per century, a rate subjected to high variations according to the conditions of preservation (Gennaretti *et al* 2014b). This indicates that the actual death date of the trees should be closer to 1816 and that the mortality caused by the Tambora (post 1815) should be likely higher than 20%, meaning four times higher than the background level. The subsequent eruptions (e.g. the 1835 Cosiguina eruption) were not associated to any detectable mortality events likely because a large portion of the most vulnerable trees had already died after the Tambora eruption.

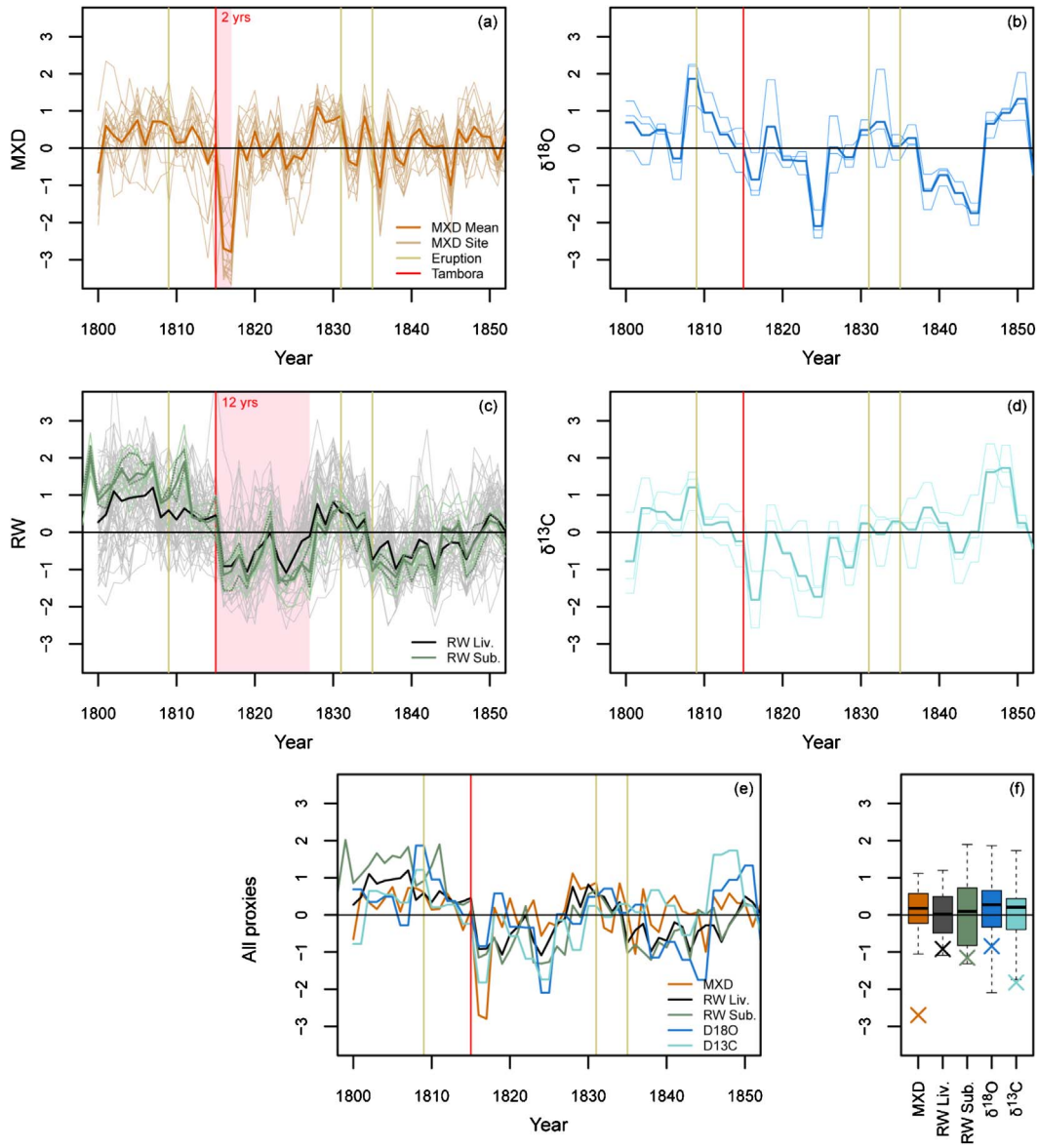

Figure 5. Tree-ring proxy time series in Eastern Canada over the 1800–1850 time period. In (*a*)–(*d*) we see single site (19 MXD chronologies in (*a*); 3 δ^{18}O chronologies in (*b*); 56 RW Liv. and 6 RW Sub. chronologies in (*c*); 3 δ^{13}C chronologies in (*d*)) and mean multisite chronologies. All data are transformed in *z*-scores. The red shadow in (*a*) and (*c*) highlights the years impacted by the Tambora. Two cambial age-specific multisite chronologies are also shown in (*c*) for the subfossil material (bold green dotted lines; cambial ages $<$ 50 years and cambial ages $>$ = 50 years). The independent multisite chronologies are compared in (*e*). The (*f*) plot shows the 1816 anomalies (crosses) relative to the distribution of the data over the 1800–1814 and 1818–1850 period (quartiles and extreme values). In (*a*)–(*e*) vertical lines are important eruption years (see table 1; Tambora is in red). MXD is ring maximum density chronologies, RW Liv. and Sub. are ring width chronologies from living and subfossil trees, respectively.

If we use the computed wood biomass production index at 19 sites as a proxy of the boreal forest aboveground carbon assimilation in eastern Canada, we can conclude that carbon dynamics are very similar to ring width variations (figure 7). This is because the coefficient of variation (ratio of the standard deviation to the mean) of the basal volume increments is nine times larger than that of wood density values (see equation 1). Consequently, the Tambora impact seems to last 12 years such as for RWs. This long-term impact is not captured by the MAIDEN simulations of black spruce GPP values during the Tambora time (figure 8). Indeed, these simulations only show one important negative anomaly in 1816 with a median percent reduction of GPP values of −11.6%. This lack of persistence is likely due to a combination of reasons: (1) the LME time series used as MAIDEN input underestimate the persistence of the Tambora impact on the regional climate (compare figures 2(*a*) and 3(*a*)); (2) the real mechanism forcing the physiological persistence of poor growth over several years two centuries ago remains unidentified and is not taken into account by ecophysiological forest models.

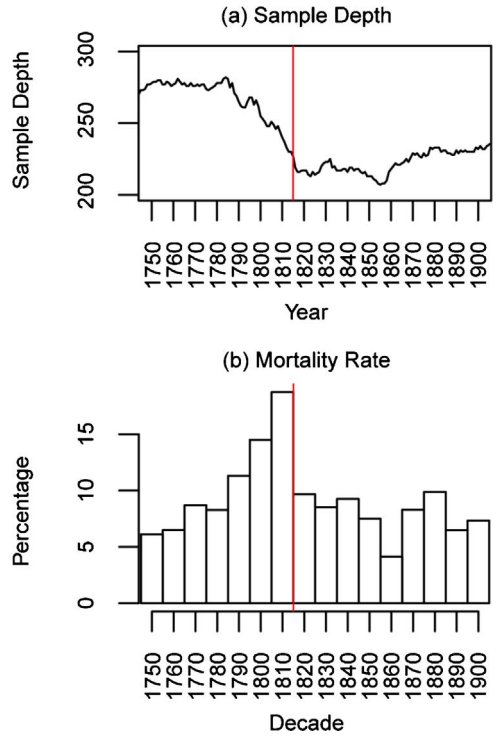

Figure 6. Sample depth ((*a*); number of trees) and tree mortality rate ((*b*); percentage of tree mortality over the total sample depth per each ten year class) in the subfossil material (all six sites). The Tambora year is the red line.

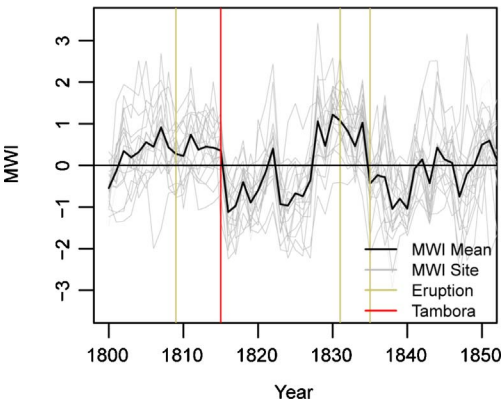

Figure 7. Wood biomass production index (MWI; values transformed in z-scores) over the 1800–1850 period at the 19 sites where both tree-ring width and density measurements are available. Vertical lines are important eruption years (see table 1; Tambora is in red).

Discussion

Our results illustrate that the legacy effects of the Tambora eruption in Eastern Canada depend on the record. There are significant differences between hydroclimate observations and the specific proxy records. The amplitude of the 1816 anomaly in the early temperature observations is similar to that in the ring width and δ^{13}C time series. In contrast, ring density records appear to be overly sensitive (figure 9), a result consistent with the findings of Tingley *et al* (2014) pointing out the impact on wood density of reduced light availability after volcanic eruptions. However, ring width and δ^{13}C values show a much longer persistence of the Tambora impact (12 years) than temperature observations (three years) and ring density (two years). Ring width records are known to have a smoothed delayed response to volcanic events (Esper *et al* 2015) because carbon dynamics in trees are generally the results of processes occurring during the current and the previous years (e.g. tree damage and recovery processes, accumulation of stored non-structural carbohydrates; see Carbone *et al* 2013). On the other hand, δ^{13}C values are a proxy of the plant intrinsic water use efficiency (Moreno-Gutiérrez *et al* 2012, Farquhar *et al* 1989, McCarroll and Loader 2004), which is directly related to the net photosynthetic rate and inversely related to the stomatal conductance. Consequently, the low δ^{13}C values after the Tambora eruption indicates a slow photosynthetic rate that lasted for some years and/or an increase of stomatal conductance after foliage losses (see Berninger *et al* 2000). These findings highlight that different biases may be present in reconstructions based on specific proxies and that multi-proxy approaches should be preferred. The post-Tambora three-year persistence detected in annual temperature observations may seem quite short because simulations studies have shown that Eastern Canada could be sensitive to strong volcanic eruptions, especially in volcanic active periods such as the early 19th century. Indeed, eruptions may be linked to the inception of longer-term feedbacks (e.g. variation in the Atlantic thermohaline circulation) determining the Atlantic multidecadal variability (Otterå *et al* 2010, Miller *et al* 2012, Schleussner and Feulner 2013). However, if we exclude tree-ring widths and isotopes, no other annually resolved observation (MXD, historical sources, river and sea-ice observations) shows a Tambora impact longer than four years in Eastern Canada (see data collected for this study and references cited in the introduction). Consequently, our results suggest a longer persistence of the Tambora signal in some specific Eastern Canada tree-ring proxy records than in the regional climate, which is in accordance with what has been found in Europe (Büntgen *et al* 2015).

Tree-ring data are excellent climate proxy records and, more specifically, are archives of changes in forest processes. Here, using our ring width and density data, we suggest that the carbon uptake of the black spruce trees in Eastern Canada was dampened for 12 years following the Tambora (figure 7). Such a long impact on forest processes is also testified by the δ^{13}C time series (figure 5). Simulation studies have already shown that volcanic perturbations are longer on land carbon pools than on global climate because of slower recovery processes (Segschneider *et al* 2013). However, our findings highlight that the Tambora legacy in Eastern Canada may be even longer than one or two decades because the eruption also triggered a massive tree mortality episode (figure 6). Consequently, the Tambora

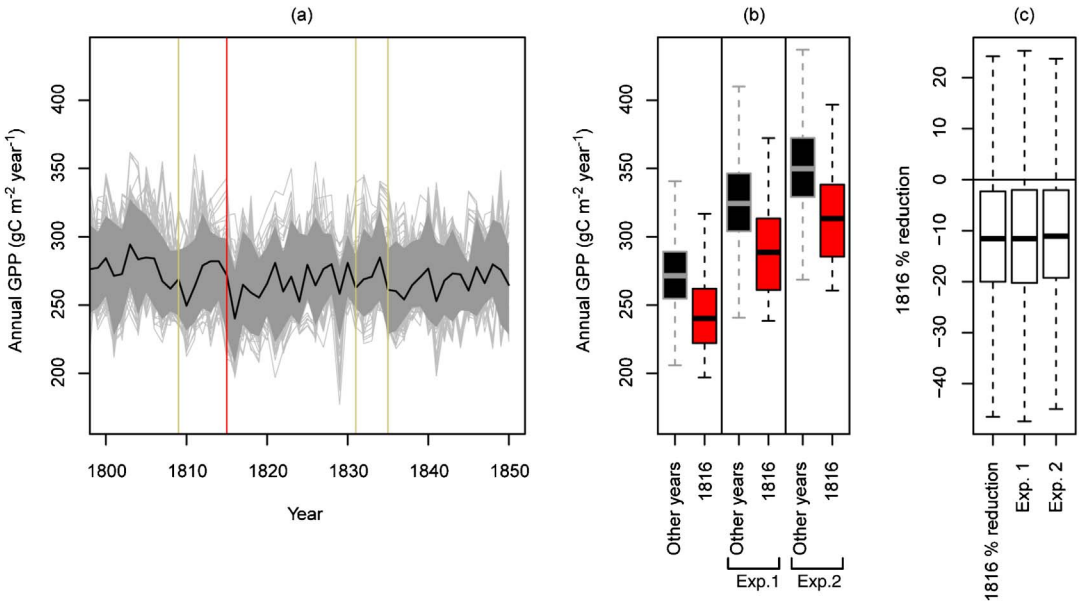

Figure 8. Black spruce forest GPP time series simulated by MAIDEN in the middle of our study region in Eastern Canada (*a*). The average of 130 simulations is shown (black line; ten simulations per each LME-member climate record sampling the MAIDEN sensitive parameters from their plausible distributions for the study region; see Gennaretti *et al* 2017) as well as the 80% confidence interval (dark grey shadow) and the outlier simulations (light grey thin lines). Vertical lines are important eruption years (see table 1, Tambora is in red). The boxes and whiskers in (*b*) show the distribution of the simulated values over the 1800–1814 and 1818–1850 period compared to the distribution for the year 1816. The GPP percent reduction in 1816 relative to the other years is shown in (*c*). In (*b*) and (*c*), the distributions obtained in the experiment 1 (fixed CO_2 concentration equal to the 1985–2005 mean) and the experiment 2 (CO_2 as in experiment 1 and temperature and precipitation time series modified by constant deltas: +0.56 °C and +0.74% respectively) are also shown.

impact on tree density could have persisted until the present because, in the study region, forest grows slowly and was almost unable to regenerate by seed during the Little Ice Age (Payette *et al* 2008). Indeed, the complete maturation of black spruce embryos needs at least 800 growing degree-days (above 5 °C; Meunier *et al* 2007), a threshold still not attained today in the center of the study region. Thus, each mortality event may be associated with a persistent shift in forest structure and composition (Gennaretti *et al* 2014a).

We suggest two complementary hypotheses to explain the mortality event and the long persistence of the Tambora impact on the forest even if more favorable climatic conditions were reestablished four-five years after the eruption. The first hypothesis is related to the occurrence of frost damages, followed by long-term recovery processes to rebuild the canopy photosynthetic capacity. This mechanism would be in part similar to that suggested by Fayle *et al* (1992). Immature shoot development during short growing seasons combined with needle and bud erosion during the cold winters in 1816-17 most likely damaged upper crowns of dominant trees, leading to growth form regression and increased stem mortality. The plausibility of this mechanism is supported by the finding of Arseneault and Payette (1997) that growth forms and ring widths of black spruce at a treeline site were severely impacted for several decades following a series of strong volcanic eruptions during the 1450s (Esper *et al* 2017). Similarly, an extended episode of tree mortality in a Labrador treeline forest stand during the early 19th century has been attributed to progressive erosion of foliage and buds by severe winter conditions (Payette 2007). The second hypothesis is related to a likely frost disturbance of the 'rootable' soil layer. The 19th century is known to be a period with intense ice-wedge and permafrost activity in Northeastern Canada (Kasper and Allard 2001). Although permafrost is generally absent from forested sites in Quebec-Labrador, due to high winter precipitation and snow retention (Payette 2001), short-term cooling events (three-four years), such as the one produced by the Tambora, could have resulted in deeper freezing and shorter frost-free season. This mechanism could have been amplified by a thin snow cover in 1816, as suggested by climate simulations (figure 3(*d*)), and by the presence of an insulating moss-*Sphagnum* mat, as it is the case in several taiga forest stands, that would have preserved the frozen soil.

Our results illustrate that the Tambora imprint in Eastern Canada is more persistent on observed data than on simulated ones (climate and forest-growth simulations). The LME mean temperature records show a stronger 1816 anomaly than climate observations (figure 9), but the low anomalies last one year only (figure 3). Indeed, at the regional level, decadal climate responses to volcanic eruptions may be controlled by the internal climate variability and by the background state of the climate system (e.g. the climatic impact of an eruption on a specific region can differ according to the preceding atmospheric and oceanic state; Zanchettin *et al* 2013). Consequently, the clear 6–10 year

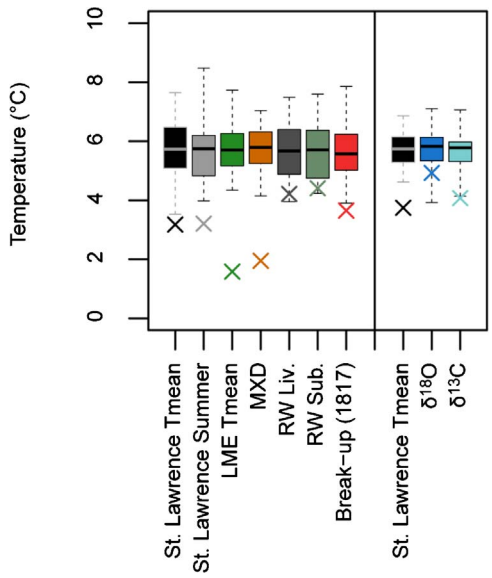

Figure 9. 1816 anomalies (crosses) in specific records: St. Lawrence Tmean and summer (July–August means) temperature values, Last Millennium Ensemble (LME) 2 m mean temperature, ring maximum density chronologies (MXD), ring width chronologies from living trees (RW Liv.), ring width chronologies from subfossil trees (RW Sub.), the mean first break-up date at Fort Albany and Moose Factory, δ^{18}O and δ^{13}C. All records are scaled to have same mean and variance than St. Lawrence Tmean over the 1800–1850 period. Boxes and whiskers show quartiles and extreme values of the data over the 1800–1814 and 1818–1850 period. For the river break-up record, the cross highlights the 1817 anomaly which is the lowest anomaly following the Tambora in this record. In the right side of the figure, the St. Lawrence Tmean record was preprocessed to have a two-year resolution and to be comparable to the δ^{18}O and δ^{13}C tree-ring records.

post-Tambora negative temperature anomalies simulated by different GCMs at the global scale (Raible *et al* 2016) are much noisier at the regional scale. The absence of a reduction of the solar flux at surface over Eastern Canada in 1816 (figure 4(*e*)) seems to represent a LME bias because reduced light availability is suggested by our observed data (ring density and δ^{13}C low values). The short-term temperature anomaly in the LME records contributed to the short-term reduction of black spruce primary production simulated by MAIDEN in the study area (figure 8). However, this short-term effect may be primarily explained by the fact that both hypotheses formulated in the previous paragraph are linked to mechanisms that are not taken into account by process-based vegetation models. Consequently, although MAIDEN is able to consider the influence of carbon stored during previous years on stand carbon dynamics (Gennaretti *et al* 2017), our GPP simulations only show a post-Tambora anomaly of one year. The 11.6% GPP reduction simulated by MAIDEN in 1816 may had partially or completely been counteracted by a concomitant reduction in soil respiration (not simulated by MAIDEN), which is known to occur in northern latitudes following volcanic eruptions (Tjiputra and Otterå 2011, Kandlbauer *et al* 2013). For all these reasons, the response of the studied boreal ecosystem in terms of net ecosystem production following the Tambora and the investigation of the mechanisms amplifying the volcanic perturbation remain interesting topics for future studies.

Ultimately, our study may help anticipate the effects of a future Tambora-like eruption on the eastern Canadian boreal forest carbon uptake. At the global scale, some simulation studies have shown that Tambora-like eruptions occurring in the 21th century could delay the upcoming warming by approximately two decades and could significantly increase the terrestrial global carbon uptake (Tjiputra and Otterå 2011, Schurer *et al* 2015). This global picture is much more uncertain at the regional scale. For our study region, we compared the 1816 GPP anomalies simulated by MAIDEN for black spruce forests (figure 8) with those simulated with modified versions of the early 19th century input climate. In the first experiment, we fixed the atmospheric CO_2 concentration data to the mean value of the 1985–2005 period (358 ppm; +74 ppm relative to 1800–1850; MacFarling Meure *et al* 2006). The simulated GPP values increased by about 50 g C m^{-2} year^{-1} (figure 8(*b*)) but the 1816 relative percent reduction (figure 8(*c*)) remained practically unchanged. In the second experiment, in addition to the CO_2 modification, we also modified the LME temperature and precipitation time series to have their 1800–1850 mean equal to their 1985–2005 mean: +0.56 °C for temperature and +0.74% for precipitation. Although these are small climatic deltas, the average GPP values increased an additional 25 g C m^{-2} year^{-1} (figure 8(*b*)). However, the 1816 relative percent reduction remained very similar and only just slightly smaller (the median values shifted from −11.6% to −11.0%; figure 8(*c*)). These analyses suggest that immediately after Tambora-like events, similar or slightly reduced impacts to those of the early 19th century can be expected on the Eastern Canada forest carbon uptake. However, the persistence of the impact and the tree mortality should be reduced in the current and future warmer climate if the triggering mechanisms are those suggested above. Furthermore, the regenerative potential of black spruce forests following disturbances is higher today than in the 19th century (Meunier *et al* 2007).

Conclusion

In this study, we collected a large amount of data from different and complementary sources over Eastern Canada, to provide an in-depth evaluation of the Tambora impact on climate and forest processes. We confirm the results of previous studies for other regions, showing that the terrestrial biosphere is much more sensitive to volcanic eruptions than the climate system. We point out that the Tambora legacy on the structure of the North American taiga could have persisted until the present. Indeed, the eruption caused a

mortality event of the dominant trees during an unfavorable period for forest regeneration. We suggest two mechanisms to explain the observed tree mortality and the persistence of the Tambora impact on the forest carbon uptake: (1) frost damages eroding the spruce growth forms; (2) deeper freezing and shorter frost-free season in the soil. These mechanisms are not considered by process-based vegetation models, which underestimate the Tambora legacy on northern ecosystems.

Acknowledgments

This project has received funding from the European Union's Horizon 2020 research and innovation programme under the Marie Sklodowska-Curie grant agreement No 656896.

ORCID iDs

Fabio Gennaretti https://orcid.org/0000-0002-8232-023X

References

Arseneault D and Payette S 1997 Reconstruction of millennial forest dynamics from tree remains in a subarctic tree line peatland *Ecology* **78** 1873–83

Autin J, Gennaretti F, Arseneault D and Bégin Y 2015 Biases in RCS tree ring chronologies due to sampling heights of trees *Dendrochronologia* **36** 13–22

Bilali H E, Patterson R T and Prokoph A 2013 A Holocene paleoclimate reconstruction for eastern Canada based on δ18O cellulose of Sphagnum mosses from Mer Bleue Bog *Holocene* **23** 1260–71

Berninger F, Sonninen E, Aalto T and Lloyd J 2000 Modeling 13 C discrimination in tree rings *Glob. Biogeochem. Cycles* **14** 213–23

Boucher E, Nicault A, Arseneault D, Bégin Y and Karami M P 2017 Decadal variations in Eastern Canada's taiga wood biomass production forced by ocean-atmosphere interactions *Sci. Rep.* **7** 2457

Briffa K R, Jones P D, Schweingruber F H and Osborn T J 1998 Influence of volcanic eruptions on Northern Hemisphere summer temperature over the past 600 years *Nature* **393** 450–5

Briffa K R, Osborn T J, Schweingruber F H, Harris I C, Jones P D, Shiyatov S G and Vaganov E A 2001 Low-frequency temperature variations from a northern tree ring density network *J. Geophys. Res. D Atmos.* **106** 2929–41

Brugnara Y *et al* 2015 A collection of sub-daily pressure and temperature observations for the early instrumental period with a focus on the 'year without a summer' 1816 *Clim. Past* **11** 1027–47

Büntgen U *et al* 2015 Tree-ring amplification of the early nineteenth-century summer cooling in central europe *J. Clim.* **28** 5272–88

Carbone M S, Czimczik C I, Keenan T F, Murakami P F, Pederson N, Schaberg P G, Xu X and Richardson A D 2013 Age, allocation and availability of nonstructural carbon in mature red maple trees *New Phytol.* **200** 1145–55

Crowley T J and Unterman M B 2013 Technical details concerning development of a 1200 year proxy index for global volcanism *Earth Syst. Sci. Data* **5** 187–97

D'Arrigo R, Buckley B, Kaplan S and Woollett J 2003 Interannual to multidecadal modes of labrador climate variability inferred from tree rings *Clim. Dyn.* **20** 219–28

Esper J, Büntgen U, Luterbacher J and Krusic P J 2013 Testing the hypothesis of post-volcanic missing rings in temperature sensitive dendrochronological data *Dendrochronologia* **31** 216–22

Esper J, Schneider L, Smerdon J E, Schöne B R and Büntgen U 2015 Signals and memory in tree-ring width and density data *Dendrochronologia* **35** 62–70

Esper J, Büntgen U, Hartl-Meier C, Oppenheimer O and Schneider L 2017 Northern Hemisphere temperature anomalies during the 1450s period of ambiguous volcanic forcing *Bull. Volcanol.* **79** 41

Fayle D C, Bentley C V and Scott P A 1992 How did treeline white spruce at Churchill, Manitoba respond to conditions around 1816 *The Year Without a Summer* (Ottawa: Canadian Museum of Nature) pp 281–90

Farquhar G D, Ehleringer J R and Hubick K T 1989 Carbon isotope discrimination and photosynthesis *Annu. Rev. Plant. Physiol. Plant. Mol. Biol.* **40** 503–37

Gao C, Robock A and Ammann C 2008 Volcanic forcing of climate over the past 1500 years: An improved ice core-based index for climate models *J. Geophys. Res. Atmos.* **113** D23111

Gea-Izquierdo G, Guibal F, Joffre R, Ourcival J M, Simioni G and Guiot J 2015 Modelling the climatic drivers determining photosynthesis and carbon allocation in evergreen Mediterranean forests using multiproxy long time series *Biogeosciences* **12** 3695–712

Gennaretti F, Arseneault D and Bégin Y 2014a Millennial disturbance-driven forest stand dynamics in the Eastern Canadian taiga reconstructed from subfossil logs *J. Ecol.* **102** 1612–22

Gennaretti F, Arseneault D and Bégin Y 2014 b Millennial stocks and fluxes of large woody debris in lakes of the North American taiga *J. Ecol.* **102** 367–80

Gennaretti F, Arseneault D, Nicault A, Perreault L and Bégin Y 2014 c Volcano-induced regime shifts in millennial tree-ring chronologies from northeastern North America *Proc. Natl Acad. Sci. USA* **111** 10077–82

Gennaretti F, Gea-Izquierdo G, Boucher E, Berninger F, Arseneault D and Guiot J 2017 Ecophysiological modeling of photosynthesis and carbon allocation to the tree stem in the boreal forest *Biogeosci.* **14** 4851–66

Guiot J 1985 Reconstruction of seasonal temperatures and sea-level pressures in the Hudson Bay area back to 1700 *Climatol. Bull.* **19** 11–59

Harington C R 1992 The year without a summer? World climate in 1816 (Ottawa: Canadian Museum of Nature)

Houle D, Moore J-D and Provencher J 2007 Ice bridges on the St. Lawrence river as an index of winter severity from 1620–1910 *J. Clim.* **20** 757–64

Hutchinson M F, McKenney D W, Lawrence K, Pedlar J H, Hopkinson R F, Milewska E and Papadopol P 2009 Development and testing of Canada-wide interpolated spatial models of daily minimum-maximum temperature and precipitation for 1961–2003 *J. Appl. Meteorol. Climatol.* **48** 725–41

Kandlbauer J, Hopcroft P O, Valdes P J and Sparks R S J 2013 Climate and carbon cycle response to the 1815 Tambora volcanic eruption *J. Geophys. Res. Atmos.* **118** 12497–507

Kasper J N and Allard M 2001 Late-Holocene climatic changes as detected by the growth and decay of ice wedges on the southern shore of Hudson Strait, northern Québec, Canada *Holocene* **11** 563–77

MacFarling Meure C, Etheridge D, Trudinger C, Steele P, Langenfelds R, van Ommen T, Smith A and Elkins J 2006 Law Dome CO_2, CH_4 and N_2O ice core records extended to 2000 years BP *Geophys. Res. Lett.* **33** L14810

McCarroll D and Loader N J 2004 Stable isotopes in tree rings *Quaternary Sci. Rev.* **23** 771–801

Meunier C, Sirois L and Bégin Y 2007 Climate and *Picea mariana* seed maturation relationships: a multi-scale perspective *Ecol. Monogr.* **77** 361–76

Miller G H *et al* 2012 Abrupt onset of the Little Ice Age triggered by volcanism and sustained by sea-ice/ocean feedbacks *Geophys. Res. Lett.* **39** L02708

Misson L 2004 MAIDEN: a model for analyzing ecosystem processes in dendroecology *Can. J. Forest Res.* **34** 874–87

Moodie D W and Catchpole A J W 1975 *Environmental Data from Historical Documents by Content Analysis: Freeze-up and Break-up of Estuaries on Hudson Bay* (Winnipeg: Department of Geography University of Manitoba) 1714–871

Moreno-Gutiérrez C, Dawson T E, Nicolás E and Querejeta J I 2012 Isotopes reveal contrasting water use strategies among coexisting plant species in a mediterranean ecosystem *New Phytol.* **196** 489–96

Naulier M, Savard M, Bégin C, Marion J, Nicault A and Bégin Y 2015 Temporal instability of isotopes–climate statistical relationships–A study of black spruce trees in northeastern Canada *Dendrochronologia* **34** 33–42

Nicault A, Boucher E, Bégin C, Guiot J, Marion J, Perreault L, Roy R, Savard M and Bégin Y 2014a Hydrological reconstruction from tree-ring multi-proxies over the last two centuries at the Caniapiscau Reservoir, northern Québec, Canada *J. Hydrol.* **513** 435–45

Nicault A *et al* 2014b Spatial analysis of the black spruce (*Picea mariana* [MILL] B.S.P.) radial growth response to climate in northern Québec, Canada *Can. J. Forest Res.* **45** 343–52

Oppenheimer C 2003 Climatic, environmental and human consequences of the largest known historic eruption: Tambora volcano (Indonesia) 1815 *Prog. Phys. Geogr.* **27** 230–59

Otterå O H, Bentsen M, Drange H and Suo L 2010 External forcing as a metronome for Atlantic multidecadal variability *Nat. Geosci.* **3** 688–94

Otto-Bliesner B L, Brady E C, Fasullo J, Jahn A, Landrum L, Stevenson S, Rosenbloom N, Mai A and Strand G 2016 Climate variability and change since 850 CE: an ensemble approach with the community earth system model *Bull. Am. Meteorol. Soc.* **97** 735–54

Payette S 2001 Les processus et les formes périglaciaires *Écologie des tourbières du Québec-Labrador. Les Presses de l'université Laval, Québec* ed S Payette and L Rochefort pp 199–239

Payette S 2007 Contrasted dynamics of northern Labrador tree lines caused by climate change and migrational lag *Ecology* **88** 770–80

Payette S, Filion L and Delwaide A 2008 Spatially explicit fire-climate history of the boreal forest-tundra (Eastern Canada) over the last 2000 years *Phil. Trans. R Soc. B Biol. Sci.* **363** 2301–16

Raible C C *et al* 2016 Tambora 1815 as a test case for high impact volcanic eruptions: Earth system effects *Wiley Interdiscip. Rev. Clim. Change* **7** 569–89

Schleussner C F and Feulner G 2013 A volcanically triggered regime shift in the subpolar North Atlantic Ocean as a possible origin of the Little Ice Age *Clim. Past* **9** 1321–30

Schurer A P, Hegerl G C and Obrochta S P 2015 Determining the likelihood of pauses and surges in global warming *Geophys. Res. Lett.* **42** 5974–82

Segschneider J, Beitsch A, Timmreck C, Brovkin V, Ilyina T, Jungclaus J, Lorenz S J, Six K D and Zanchettin D 2013 Impact of an extremely large magnitude volcanic eruption on the global climate and carbon cycle estimated from ensemble earth system model simulations *Biogeosciences* **10** 669–87

Self S, Gertisser R, Thordarson T, Rampino M and Wolff J 2004 Magma volume, volatile emissions, and stratospheric aerosols from the 1815 eruption of tambora *Geophys. Res. Lett.* **31** L20608

Sigl M *et al* 2013 A new bipolar ice core record of volcanism from WAIS Divide and NEEM and implications for climate forcing of the last 2000 years *J. Geophys. Res. Atmos.* **118** 1151–69

Sigl M *et al* 2015 Timing and climate forcing of volcanic eruptions for the past 2, 500 years *Nature* **523** 543–9

Slonosky V 2014 Historical climate observations in Canada: 18th and 19th century daily temperature from the St. Lawrence Valley, Quebec *Geosci. Data J.* **1** 103–20

Slonosky V C 2015 Daily minimum and maximum temperature in the St-Lawrence Valley, Quebec: two centuries of climatic observations from Canada *Int. J. Climatol.* **35** 1662–81

Suffling R and Fritz R 1992 *The Ecology of a Famine: Northwestern Ontario in 1815–17* ed C Harington (Ottawa: Canadian Museum of Nature) pp 203–17

Tingley M P, Stine A R and Huybers P 2014 Temperature reconstructions from tree-ring densities overestimate volcanic cooling *Geophys. Res. Lett.* **41** 7838–45

Tjiputra J F and Otterå O H 2011 Role of volcanic forcing on future global carbon cycle *Earth Syst. Dyn.* **2** 53–67

Vallée S and Payette S 2004 Contrasted growth of black spruce (*Picea mariana*) forest trees at treeline associated with climate change over the last 400 years *Arctic Antarct. Alpine Res.* **36** 400–6

Viau A E, Ladd M and Gajewski K 2012 The climate of North America during the past 2000 years reconstructed from pollen data *Glob. Planet Change* **84** 75–83

Wagner S and Zorita E 2005 The influence of volcanic, solar and CO_2 forcing on the temperatures in the dalton minimum 1790–1830: a model study *Clim. Dyn.* **25** 205–18

Wilson C 1992 Climate in Canada, 1809-20: three approaches to the Hudson's Bay company archives as an historical database *The Year Without a Summer* (Ottawa: Canadian Museum of Nature) 162–84

Zanchettin D, Bothe O, Graf H F, Lorenz S J, Luterbacher J, Timmreck C and Jungclaus J H 2013 Background conditions influence the decadal climate response to strong volcanic eruptions *J. Geophys. Res. D Atmos.* **118** 4090–106